Nanoscale

Accepted Manuscript

Journal Name

COMMUNICATION

Observation of polarized gain from aligned colloidal nanorods

Yuan Gao, [a,b] Van Duong Ta, [b] Xin Zhao, [a,b] Yue Wang, [a] Rui Chen, [a] Evren Mutlugun, [a,b,c] Kah Ee Fong, [b] Swee Tiam Tan, [b] Cuong Dang, [b] Xiao Wei Sun, [b] Handong Sun, *[a,b] and Hilmi Volkan Demir*[a,b,d]

Colloidal semiconductor nanorods have attracted great interest for polarized spontaneous emission in recent years. However, their polarized gain has not been possible to date. In this work we show highly polarized stimulated emission from the densely packed ensembles of core-seeded nanorods in a cylindrical cavity. Here CdSe/CdS dot-in-rods were coated and aligned on the inner wall of a capillary tube providing optical feedback for the nanorod gain medium. Results show that the polarized gain originates intrinsically from the aligned nanorods and not from the cavity and that the optical anisotropy of the nanorod ensemble was amplified with the capillary tube, resulting in highly polarized whispering gallery mode lasing. The highly polarized emission and lasing, together with easy fabrication and flexible incorporation, make this microlaser promising for important color conversion and enrichment applications including liquid crystal display backlighting and laser lighting.

Semiconductor nanocrystals are attractive materials offering numerous applications ranging from bioimaging[1] to optoelectronic devices including, light emitting diodes(LEDs)[2], solar cells[3] and lasers[4, 5]. Over the past thirty years, the development of colloidal nanocrystals has led to the achievement of high photoluminescence (PL) quantum yields with narrow emission linewidths as well as tunability of the peak emission wavelength from the ultraviolet to the infrared by tailoring the size, structure and/or chemical composition.[6] Additionally, solution-based processing of these colloidal semiconductor nanoparticles has allowed for low cost fabrication, essentially at any substrate, for diverse photonic devices.

Given the nanoscale size of semiconductor nanoparticles, their density of electronic states is atomic-like because of the quantum confinement effect, which makes the emission wavelength and optical gain of this material class less sensitive to temperature.[4] Meanwhile, their better photostability compared to organic dyes combined with their rare earth element free nature makes nanocrystals promising for potential applications in lasers.[7]

Lasing from semiconductor nanocrystals was first demonstrated in 1991, by optical pumping CdSe nanocrystal doped glass at 80 K.[8] However, under strong excitation that creates multiexcitons, Auger recombination becomes an undesired nonradiative channel, a competing process for stimulated emission.[9-11] In order to suppress the Auger recombination, the concept of single exciton gain was introduced and realized by using type-II nanocrystals where electrons and holes are distributed separately in cores and shells of the semiconductor nanocrystals.[12] However, adopting type-II nanocrystals leads to an extreme reduction in the overlap of

electron and hole wave functions so that the emission transition rate is decreased significantly. In addition, recent type-I nanocrystal lasers operating in single exciton regime require relatively low pumping intensity to avoid multiexciton Auger loss but this also limits their output power.[12] Suppressing Auger recombination rate, while maintaining the optical oscillation strength by engineering electron hole wave-functions, has been a subject of studies in various nanocrystal structures.[13-16]

A new type of semiconductor heterostructure nanocrystals in a rod shape, CdSe core-seeded CdS nanorods, or CdSe/CdS dot-in-rods (DRs), has been recently synthesized.[13] CdSe/CdS DRs preserve the conventional nanocrystals' discrete electronic states and exhibit nearly temperature independent threshold.[17] On the other hand, the offset of conduction band is very small in comparison to that of valence band.[18] Therefore, holes are mainly confined in the CdSe core while electrons spread in the whole CdS rod. Because of their quasi-type-II band alignment, CdSe/CdS DRs show a pronounced reduction of Auger recombination and remarkable increase of gain lifetime.[16, 19-22] Given the temperature insensitive threshold and suppression of Auger recombination, CdSe/CdS DRs are promising candidates for optical gain applications.

On the other hand, polarized light is essential to liquid-crystal display (LCD) and 3D display technologies. Polarized emission was previously observed from elongated semiconductor nanocrystals.[23] As asymmetric nanocrystals with mixed dimensionality, CdSe/CdS DRs not only preserve the merits of spherical nanocrystals such as wide color tunability but also show anisotropic properties of absorption and emission.[13, 24-26] To utilize such anisotropic optical properties for photonic devices, CdSe/CdS DRs must be oriented in a collective way. Many efforts have been made to realize

nanocrystal superlattices in a large scale to enable anisotropic emission from nanorod ensembles such as self-assembling on water surface,[27] controlled evaporation,[28] electric field assisted alignment,[13, 29] and others. However, these approaches have typically been limited to monolayers with anisotropic fluorescence and have not been able to achieve optical gain to date.

Capillary tube is a good host for possible gain medium since it can play the role of a cylindrical optical microcavity along with the generation of whispering gallery modes (WGM) to provide optical feedback.[30, 31] The tubes are usually filled with optical gain solutions. However, low refractive index contrast between the solution and glass tube reduces the overlap of optical modes with gain medium, which makes it difficult to lase.[30, 31] Beside the low refractive index contrast and low density problem, randomly distributed DRs in solution cannot utilize their anisotropic dipole moment for the optical gain.

In this work, in order to address all of these outlined problems, we show the first account of the high-density packing of DRs aligned with a preferable orientation in large scale to enable strong polarized gain medium. Here CdSe/CdS core-seeded nanorods were used to be aligned with the capillary tubes and cover their inner walls, forming a collective effect in the cylindrical microcavity. Spontaneous emission with very high polarization ratio was observed to confirm the preferable orientation of the CdSe/CdS DR ensemble in the capillary tubes. Unlike WGM lasing with an isotropic gain medium in a cylindrical cavity of hundreds of micrometer in diameter, where the cavity shows negligible polarization selectivity,[30, 32] the WGM lasing with the polarized gain medium of these aligned CdSe/CdS DRs was strongly polarized.

CdSe/CdS DRs were synthesized with a seeded growth approach.[13] The photoluminescence quantum yield is 0.75 determined by comparison with Rhodamine 101 in ethanol.[33] The first absorption peak and the PL emission spectrum of CdSe quantum dot and CdSe/CdS DR solution show very well defined exciton peaks of the quantum dot structure (Fig. S1). Absorption cross section is increased dramatically at shorter wavelength after CdS rod growth (Fig. S1a). This helps harvesting more pump photons and facilitates population inversion for stimulated emission.[34]

To verify the intrinsic anisotropy in optical properties of CdSe/CdS DRs, the fluorescence anisotropy was measured for diluted CdSe/CdS DR solution in a cuvette. A continuous wave laser with 532 nm wavelength and linear polarization was used as an excitation source in the experimental setup, shown in Fig. 1a. Fig. 1b presents the fluorescence spectra of DR solution at two different polarizations, which are parallel and perpendicular to the excitation polarization, respectively. As we can see, the DR solution tends to emit photons in the same polarization with that of the excitation source. Fig. 1c shows the integrated fluorescence intensity from the DR solution at different polarization angles (θ) with respect to the excitation polarization. The fitting curve shows the $cos^2\theta$ behavior of the emission intensity. In contrast, the diluted spherical wurtzite CdSeS/ZnS nanocrystal solution showed isotropic emission (Fig. S2a). Similar experiments were also repeated with a zinc blende spherical shaped CdSe/CdS/ZnS nanocrystal solution where no anisotropic fluorescence was observed, ruling out the effects of crystalline structure (Fig. S2b). This anisotropic emission from CdSe/CdS DRs revealed the difference in dipole moments between the orientations which are along (μ_c) and normal (μ_a, μ_b) to the DRs' long axis. The fluorescence anisotropy is defined as $r=(I_{//} - I_\perp)/(I_{//} + 2I_\perp)$,[29] where $I_{//}$ and $I_\perp$

are the emission intensities with polarizations in parallel and perpendicular direction of excitation polarization, respectively. In spherical quantum dot ensembles, the dipole moments are equal in all 3 dimensions ($\mu_a= \mu_b= \mu_c$), the fluorescence anisotropy r = 0. While the fluorescence anisotropy values are 0.4 and 0.1 for the ensembles of ideal nanorod ($\mu_a= \mu_b<< \mu_c$) and ideal nanodisk ($\mu_a= \mu_b>>\mu_c$), respectively, as presented in Fig. 1d and supporting information. Our DR solution shows the fluorescence anisotropy r = 0.12, which corresponds to $\mu_a=\mu_b=0.46\mu_c$. This anisotropy in the dipole moments will be utilized in our aligned DR structures.
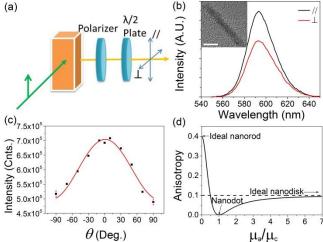

Fig. 1 Fluorescence anisotropy measurement of diluted CdSe/CdS DRs solution. (a) Measurement configuration for fluorescence anisotropy. The polarizer was used to select the fluorescence with desired polarization. The achromatic half-wave plate was used to tilt the polarization of the emission horizontally before detection. (b) Spectra of emission from diluted CdSe/CdS DR solution with two different polarizations, which were parallel and perpendicular to the excitation polarization. The inset shows the high resolution transmission electron microscopy (TEM) image of a single CdSe/CdS DR (scale bar, 10 nm). (c) Emission intensity of diluted CdSe/CdS DR solution at different polarization angles with respect to the excitation polarization. (d) Fluorescence anisotropy as a function of the ratio between dipole moments for a fluorescent material with cylindrical symmetry ($\mu_a= \mu_b \neq \mu_c$).

CdSe/CdS DRs were dissolved in hexane (5 mg/mL), and solution was loaded in capillary tubes by capillary forces. The capillary tubes with diameter of 300 μm loaded with DR solution were dried under reduced pressure or in atmosphere. As the result, DRs were deposited on the inner wall of the capillary tube. Two methods were employed to verify the optical anisotropy of the DR ensemble in the capillary tubes (Fig. 2). The first method, as illustrated in Fig. 2b, uses a linear polarized laser to excite the sample, and while tuning the polarization angle of the excitation beam with respect to capillary tube's axis, the PL spectra of the DRs loaded in capillary were recorded. In the second approach, the sample was excited with a circularly polarized laser, and the polarization of PL was analyzed by varying the angle of polarizer with respect to the capillary tube's axis before detection, as shown in Fig. 2c. These two methods are basically used to examine the polarization dependent absorption and emission of CdSe/CdS DR ensemble in capillary tube by means of varying the excitation and emission detection polarization angle, respectively. If the DRs are randomly oriented, i.e., their dipole moments are evenly distributed at all angles, the absorption and emission of CdSe/CdS DR ensemble will not be

Fig. 2 Two approaches that adopted for anisotropic absorption and emission measurement. (a) Cross section of capillary tube with dried CdSe/CdS DRs layer on its inner wall. (b) Excitation by linear polarized light for anisotropic absorption measurement: varying the polarization angle of excitation and monitoring the emission. (c) Excitation by circularly polarized light for anisotropic emission measurement: varying the polarization angle of the polarizer before detector and monitoring the emission. (d-e) Normalized emission intensity of spontaneous emission as a function of the polarization angle with respect to the capillary tube in the two approaches for capillary tube loaded with dried CdSe/CdS DRs (d) and CdSeS/ZnS spherical nanocrystals (e).

polarization dependent. Fig. 2d presents the PL intensity of DR ensemble as functions of excitation and emission detection polarization angles with respect to the capillary tube's axis corresponding to the two experiments. The results show that the preferable orientation for polarization of both absorption and emission is parallel to the capillary tube's axis. The same measurements were applied to the spherical nanocrystal ensemble in capillary, as shown in Fig. 2e. Polarization dependent absorption and emission for spherical nanocrystals dried in capillary tube are negligible compared to that of DRs. In addition, the anisotropic behavior was observed when the microcavity was broken by cracking the capillary tubes (Fig. S3). Hence, the effect of the cylindrical microcavity to the anisotropic optical properties is ruled out, similar to other reports about large cylindrical microcavity.[32] The data points were well fitted with cosine-squared function of polarization angle (Fig. 2d): $cos^2\theta$, where θ is angle between the capillary tube axis and the polarization of excitation or emission corresponding to our first or second method. The polarization ratio to characterize the degree of optical anisotropy of DR ensemble in capillary tubes is defined as $p=(I_{//} - I\perp)/(I_{//} + I\perp)$, where $I_{//}$ and $I\perp$ are the intensities of PL emission with polarization of excitation (or emission) parallel and perpendicular to the capillary tube, respectively. The

polarization ratios calculated based on the fitting curves in Fig. 2d, are 0.252 and 0.296 for emission and absorption, respectively. As shown above, individual CdSe/CdS DRs demonstrate highest transition probability of absorption and emission along their c-axis; the high polarization ratios of DR ensemble indicate that the DRs have a preferable orientation along the capillary tube. This is also statistically illustrated by scanning electron microscopy (SEM) images of the sample as shown in Fig. S4.

Furthermore, the collective effects with stimulated emission of the aligned DRs in the capillary tubes were investigated. A more concentrated (10 mg/mL) CdSe/CdS DRs solution was loaded in the capillary tube to deposit onto the inner wall of capillary tube a preferable film for stimulated emission. The circularly polarized laser, generated from a frequency-doubled Nd:YAG pulsed laser at 532 nm with a repetition rate of 60 Hz and a pulse width of 1 ns and a quarter-wave plate, was used to excite the sample, and the emission anisotropy was examined by varying the polarizer before detection, as shown in Fig. 2c. Under low excitation energy, the emission from the sample was observed as spontaneous emission with full a width at half maximum (FWHM) of about 34 nm, which is similar to those in above experiments. Increasing the pump energy above the threshold, the emission spectrum became narrow and series of

spiky peaks emerged, as shown in Fig. 3a. Closely investigating the lasing peaks (Fig. 3b), the peaks that are equally spaced with $\delta\lambda$=0.21 nm can be resolved (Fig. 3c). The difference of $\delta\lambda$ between the TE mode (where the electric field is perpendicular to tube axis, i.e., -90° or 90°) and the TM mode (where the electric field is parallel to tube axis, i.e., 0°) is negligible. These well resolved lasing modes also suggest the optically smooth gain medium with negligible scattering, which is consistent with SEM image of the CdSe/CdS DR layer on the inner wall of capillary tube (Fig. S4d). As a comparison given in supporting Fig. S5, the mode spacing ($\delta\lambda$) in the similar lasing structure with a smaller capillary tube diameter of 100 μm is $\delta\lambda$=0.59 nm, three times of that in 300 μm capillary tube diameter. This result confirms the WGMs in our cylindrical microcavities. For WGMs, $\delta\lambda=\lambda^2/(2\pi nR)$, where the center emission wavelength is λ=620 nm, and the capillary tube radius is R=150 μm, so the effective refractive index n is about 1.92. Such high refractive index suggests the lasing modes had a large overlap with closely packed CdSe/CdS DR layers. The high refractive index contrast between the dense semiconductor nanocrystal layers and the glass in comparison to that between organic solvent and glass creates a desired laser configuration where the overlapping between optical modes and the gain medium can be maximized. Fig. 3b also shows the different intensities of lasing spectra in TM and TE modes. As we can see, lasing intensity in TM mode was much higher than that of TE mode lasing. The lasing intensity, integral of all the lasing peaks from 615 to 625 nm, as a function of the polarization angle was measured and shown in Fig. 3d under 7 μJ pump energy. As comparison, the same measurement was conducted with spherical CdSeS/ZnS nanocrystals dried in capillary tube, as shown in Fig. S6, and the emission normal to the capillary tube was slightly stronger than that along the capillary. This is due to the light which is polarized normal to the axis of capillary tube is more likely to transmit out. The results show the anisotropy of lasing emission in our laser configuration resulted from aligned DRs.
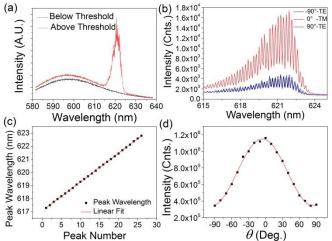

Fig. 3 Stimulated emission characterization from CdSe/CdS DRs in capillary tube. (a) Emission of DRs in capillary tube below and above the lasing threshold. (b) Spectra of lasing pumped by a circularly polarized laser from CdSe/CdS DRs in capillary when the detected polarization is along the tube (0°, TM mode) and perpendicular (-90° and 90°, TE mode). (c) Plot of laser peaks versus the peak number and linear fit of the data. (d) Lasing intensity as a function of the detection angle with respect to the capillary tube, and fitted with $cos^2\theta$ function.

Fig. 4a presents the power transfer functions measured for TE and TM modes of our laser structure. The results are well

consistent with "soft threshold" approximation[35], and threshold was about 5.2 μJ for both TE and TM modes. As can be seen, initially the difference of lasing intensity between these two modes is small, and then it grows as increasing pumping energy. The evolution of polarization ratio, p, as a function of pump energy was plotted in Fig. 4b. The polarization ratio of spontaneous emission started at about 0.05 and as the pumping energy increased, the polarization ratio built up and finally saturated at 0.72. Here, we notice that the polarization ratio reduction in spontaneous emission of this thicker DR film in comparison to the one in Fig. 3. The increase of reabsorption in a thicker film could be the main reason for this polarization ratio reduction. However, majority of CdSe/CdS DRs is oriented along the capillary tube, creating a polarized gain medium with a higher gain coefficient for amplifying light with electric vector along the tube. The small anisotropy of spontaneous emission is amplified in the polarized gain medium[36] and resulted in a very large polarization ratio p= 0.72.
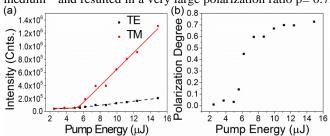

Fig. 4 Power transfer function of CdSe/CdS DRs in a capillary tube. (a) With increasing the pump energy, the evolution of lasing intensity, integral of all the lasing peaks, for TE and TM WGMs lasing, respectively. (d) Polarization ratio as a function of pump energy.

Conclusions

In summary, we demonstrated the utilization of intrinsic optical anisotropy of CdSe/CdS DRs in a large scale both for spontaneous and stimulated emissions for the first time. Evaporating CdSe/CdS DR solution inside a capillary tube leaves a thin film of aligned DRs on the inner wall of the tube. The polarization ratio of spontaneous absorption and emission for aligned DR films are 0.296 and 0.252, respectively, while the WGM lasing resulted from the cylindrical microcavity has the maximum polarization ratio of 0.72. Capillary tubes, after sealing in inert gas, also serve as oxygen and moisture free containers for CdSe/CdS DRs. Therefore, the lifetime and stability of these lasers can be much improved. Recently, LCD TVs were developed with nanocrystals in capillary tubes as the color convertors.[37] Given stimulated emission at red, green and blue color can be observed from CdSe/CdS DRs,[17] our approach with the capillary tubes demonstrating laser emission with high polarization ratio could be realized for novel display backlighting and laser lighting applications[38].

Experimental methods

Synthesis of CdSe/CdS dot-in-rods: The synthesis approach is adopted from literature.[13] For CdSe seed synthesis, 3 g trioctylphosphine oxide (TOPO), 280 mg octadecylphosphonic acid (ODPA), and 60 mg cadmium oxide (CdO) were added in a 50 mL three-neck flask. Subsequently the mixture was degased at 150 °C for 2 hrs. As the temperature was increased in Ar atmosphere, 1.8 mL trioctylphosphine (TOP) were added after CdO dissolved completely. 58 mg selenium in 0.36 g TOP were injected when the temperature reached 380 °C. Then the

flask was removed from the heat mantle intermediately. As for the seeded nanorod growth, 3 g TOPO, 290 mg ODPA, 80 mg hexylphosphonic acid (HPA) and 86 mg CdO were degased under vacuum for 2 hrs in a three-neck flask at 150 ℃. 1.8 mL TOP were added into the reaction vessel after the mixture became transparent, and then 200 μl CdSe seeds (400 μM in TOP) together with 120 mg sulfur in 1.5 g TOP were injected swiftly at 350 ℃. The as-synthesized CdSe/CdS DRs were cleaned with acetone and methanol, then dissolved in hexane. Wurtzite and zinc blende spherical nanocrystal synthesis were synthesized with one-pot [39] and successive ion layer adsorption and reaction (SILAR) [40] method, respectively.

Optical characterization: Absorption and PL spectra were measured with UV-1800 Shimadzu and RF-5301 PC. Continuous wave frequency doubled Nd:YAG laser at 532 nm was used for anisotropic optical properties measurement of DRs solution and loaded in capillary tubes. For lasing characterization, sample was pumped by frequency doubled Nd:YAG pulsed laser at 532 nm, whose repetition rate is 60 Hz and pulse width is 1 ns. Meanwhile, the polarization response of the detector was measured and corrected, and the detection system shows very good polarization insensitivity (Fig. S7).

Acknowledgements

Notes and references

a Division of Physics and Applied Physics, School of Physical and Mathematical Sciences, Nanyang Technological University, 21 Nanyang Link, 637371, Singapore. Fax: 65 6316 6984; Tel: 65 6790 5395; Email: hdsun@ntu.edu.sg (HD Sun) or hvdemir@ntu.edu.sg (HV Demir)
b LUMINOUS! Center of Excellence for Semiconductor Lighting and Displays, School of Electrical and Electronic Engineering, Nanyang Technological University, 50 Nanyang Avenue, 639785, Singapore.
c Presently at Department of Electrical and Electronics Engineering, Abdullah Gul University, 38039, Melikgazi, Kayseri.
d Department of Electrical and Electronics Engineering and Department of Physics, UNAM – Institute of Materials Science and Nanotechnology, Bilkent University, Bilkent, Ankara, Turkey; Email: volkan@bilkent.edu.tr
† Electronic Supplementary Information (ESI) available: absorption and photoluminescence spectra, calculation of anisotropy, optical and electron microscopy images, lasing characterization, and polarization response of the detectors. See DOI: 10.1039/b000000x/

1. M. Bruchez, M. Moronne, P. Gin, S. Weiss and A. P. Alivisatos, *Science*, 1998, **281**, 2013-2016.
2. J. Caruge, J. Halpert, V. Wood, V. Bulović and M. Bawendi, *Nature Photonics*, 2008, **2**, 247-250.
3. E. H. Sargent, *Nature Photonics*, 2012, **6**, 133-135.
4. V. Klimov, A. Mikhailovsky, S. Xu, A. Malko, J. Hollingsworth, C. Leatherdale, H.-J. Eisler and M. Bawendi, *Science*, 2000, **290**, 314-317.
5. J. Q. Grim, S. Christodoulou, F. Di Stasio, R. Krahne, R. Cingolani, L. Manna and I. Moreels, *Nature nanotechnology*, 2014, **9**, 891-895.
6. D. V. Talapin, J.-S. Lee, M. V. Kovalenko and E. V. Shevchenko, *Chemical reviews*, 2009, **110**, 389-458.
7. T. Erdem and H. V. Demir, *Nature Photonics*, 2011, **5**, 126-126.
8. Y. V. Vandyshev, V. Dneprovskii and V. Klimov, *JETP Letters*, 1991, **53**, 314.
9. V. Klimov, A. Mikhailovsky, D. McBranch, C. Leatherdale and M. Bawendi, *Science*, 2000, **287**, 1011-1013.
10. F. Garcá-Santamará, Y. Chen, J. Vela, R. D. Schaller, J. A. Hollingsworth and V. I. Klimov, *Nano letters*, 2009, **9**, 3482-3488.
11. L.-W. Wang, M. Califano, A. Zunger and A. Franceschetti, *Physical review letters*, 2003, **91**, 056404.
12. V. I. Klimov, S. A. Ivanov, J. Nanda, M. Achermann, I. Bezel, J. A. McGuire and A. Piryatinski, *Nature*, 2007, **447**, 441-446.
13. L. Carbone, C. Nobile, M. De Giorgi, F. D. Sala, G. Morello, P. Pompa, M. Hytch, E. Snoeck, A. Fiore and I. R. Franchini, *Nano letters*, 2007, **7**, 2942-2950.
14. B. Guzelturk, Y. Kelestemur, M. Z. Akgul, V. K. Sharma and H. V. Demir, *The Journal of Physical Chemistry Letters*, 2014.
15. B. Guzelturk, Y. Kelestemur, M. Olutas, S. Delikanli and H. V. Demir, *ACS nano*, 2014.
16. Y. Kelestemur, A. F. Cihan, B. Güzeltürk and H. V. Demir, *Nanoscale*, 2014.
17. I. Moreels, G. Rainò, R. Gomes, Z. Hens, T. Stöferle and R. F. Mahrt, *Advanced Materials*, 2012, **24**, OP231-OP235.
18. C. Grivas, C. Li, P. Andreakou, P. Wang, M. Ding, G. Brambilla, L. Manna and P. Lagoudakis, *Nature communications*, 2013, **4**.
19. M. Zavelani-Rossi, M. G. Lupo, F. Tassone, L. Manna and G. Lanzani, *Nano letters*, 2010, **10**, 3142-3150.
20. Y. Wang, V. D. Ta, Y. Gao, T. C. He, R. Chen, E. Mutlugun, H. V. Demir and H. D. Sun, *Advanced Materials*, 2014, **26**, 2954-2961.
21. M. Zavelani-Rossi, M. G. Lupo, R. Krahne, L. Manna and G. Lanzani, *Nanoscale*, 2010, **2**, 931-935.
22. F. Pisanello, G. Leménager, L. Martiradonna, L. Carbone, S. Vezzoli, P. Desfonds, P. D. Cozzoli, J.-P. Hermier, E. Giacobino, R. Cingolani, M. De Vittorio and A. Bramati, *Advanced Materials*, 2013, **25**, 1974-1980.
23. J. Hu, L.-s. Li, W. Yang, L. Manna, L.-w. Wang and A. P. Alivisatos, *Science*, 2001, **292**, 2060-2063.
24. J. S. Kamal, R. Gomes, Z. Hens, M. Karvar, K. Neyts, S. Compernolle and F. Vanhaecke, *Physical Review B*, 2012, **85**, 035126.
25. F. Pisanello, L. Martiradonna, G. Leménager, P. Spinicelli, A. Fiore, L. Manna, J.-P. Hermier, R. Cingolani, E. Giacobino and M. De Vittorio, *Applied physics letters*, 2010, **96**, 033101.
26. A. Sitt, A. Salant, G. Menagen and U. Banin, *Nano letters*, 2011, **11**, 2054-2060.
27. A. Rizzo, C. Nobile, M. Mazzeo, M. D. Giorgi, A. Fiore, L. Carbone, R. Cingolani, L. Manna and G. Gigli, *ACS nano*, 2009, **3**, 1506-1512.
28. J. L. Baker, A. Widmer-Cooper, M. F. Toney, P. L. Geissler and A. P. Alivisatos, *Nano letters*, 2009, **10**, 195-201.
29. K. M. Ryan, A. Mastroianni, K. A. Stancil, H. Liu and A. Alivisatos, *Nano letters*, 2006, **6**, 1479-1482.
30. M. Kazes, D. Y. Lewis, Y. Ebenstein, T. Mokari and U. Banin, *Advanced Materials*, 2002, **14**, 317-321.

31. Y. Wang, K. S. Leck, V. D. Ta, R. Chen, V. Nalla, Y. Gao, T. He, H. V. Demir and H. Sun, *Advanced Materials*, 2014.

32. N. Frateschi, A. Kanjamala, A. Levi and T. Tanbun-Ek, *Applied physics letters*, 1995, **66**, 1859-1861.

33. M. Grabolle, M. Spieles, V. Lesnyak, N. Gaponik, A. Eychmu□ller and U. Resch-Genger, *Analytical Chemistry*, 2009, **81**, 6285-6294.

34. G. Xing, Y. Liao, X. Wu, S. Chakrabortty, X. Liu, E. K. Yeow, Y. Chan and T. C. Sum, *ACS nano*, 2012, **6**, 10835-10844.

35. J. Herrnsdorf, B. Guilhabert, Y. Chen, A. Kanibolotsky, A. Mackintosh, R. Pethrick, P. Skabara, E. Gu, N. Laurand and M. Dawson, *Optics express*, 2010, **18**, 25535-25545.

36. B. E. A. Saleh and M. C. Teich, *Fundamentals of Photonics*, Wiley, 2013.

37. R. J. Nick, C. A. BREEN, C. M. Denton, S. Sadasivan and J. R. Linton, Google Patents, 2014.

38. A. Neumann, J. J. Wierer, W. Davis, Y. Ohno, S. R. Brueck and J. Y. Tsao, *Optics express*, 2011, **19**, A982-A990.

39. W. K. Bae, J. Kwak, J. Lim, D. Lee, M. K. Nam, K. Char, C. Lee and S. Lee, *Nano letters*, 2010, **10**, 2368-2373.

40. O. Chen, J. Zhao, V. P. Chauhan, J. Cui, C. Wong, D. K. Harris, H. Wei, H.-S. Han, D. Fukumura and R. K. Jain, *Nature materials*, 2013, **12**, 445-451.